

## ORIGINAL RESEARCH ARTICLE

## Innovative infrared imaging approach for breast cancer screening: Integrating rotational thermography and machine learning analysis

Asok Bandyopadhyay<sup>1†\*</sup> , Himanka S. Mondal<sup>1†</sup>, Bivas Dam<sup>2</sup>,  
Dipak C. Patranabis<sup>2</sup>, and Barnali Pal<sup>1</sup><sup>1</sup>ICT&SERVICES Group, Centre for Development of Advanced Computing, Kolkata, West Bengal, India<sup>2</sup>Department of Instrumentation and Electronics, Jadavpur University, Kolkata, West Bengal, India

## Abstract

This paper presents a novel approach to breast cancer screening using infrared (IR) imaging. This work encompasses four phases: Refining data collection, advancing analysis methods, and enhancing feature extraction with machine learning. The developed system employed a temperature-controlled chamber with rotational thermography techniques to maintain consistent temperatures and capture high-quality IR images and all possible subject views. The paper describes four key experiments to detect breast cancer using IR imaging. The experiments involved the use of dynamic temperature-based data collection and a semi-circular arc movement to ensure precise imaging, keeping the object in focus. Initial experiments involved the use of dynamic temperature-based data collection and a semi-circular arc movement to ensure precise imaging focus. The final experiment incorporated a semi-circular arc movement. For each subject, 32 thermal IR images were acquired, targeting one breast at a time while isolating the other with an IR-proof barrier. The collected datasets were used for breast abnormality detection. The analyzed results revealed that support vector machine and neural network algorithms achieved an accuracy rate of 93.18%. The system's installation at a hospital in India allowed for real-world application and validation. The final study, which introduced a new IR imaging protocol, demonstrated improved results compared to earlier pilot studies. This method enhances the accuracy of distinguishing malignant and benign tumors, supporting early breast cancer detection and treatment. The proposed methodology addresses data collection and analysis challenges, leading to improved screening efficiency and better patient outcomes.

<sup>†</sup>These authors contributed equally to this work.

**\*Corresponding author:**Asok Bandyopadhyay  
(b\_ashoke@hotmail.com)

**Citation:** Bandyopadhyay A, Mondal HS, Dam B, Patranabis DC, Pal B. Innovative infrared imaging approach for breast cancer screening: Integrating rotational thermography and machine learning analysis. *Artif Intell Health*. 2024;1(3):64-79.  
doi: 10.36922/aih.3312

**Received:** March 28, 2024**Accepted:** May 24, 2024**Published Online:** July 23, 2024**Copyright:** © 2024 Author(s).

This is an Open-Access article distributed under the terms of the Creative Commons Attribution License, permitting distribution, and reproduction in any medium, provided the original work is properly cited.

**Publisher's Note:** AccScience Publishing remains neutral with regard to jurisdictional claims in published maps and institutional affiliations.

**Keywords:** Infrared technology; Thermal imaging; Breast cancer screening; Dynamic data; Data collection methods; Rotational thermography

## 1. Introduction

Infrared (IR) technology-based imaging has emerged as a versatile medical imaging technique, facilitating the capture of temperature distributions across the human body's surface. IR imaging has gained attention in medical diagnosis by complementing other imaging methods. Notably, studies have highlighted a correlation between malignant

breast tumors and elevated temperatures, prompting consideration of IR imaging as a valuable tool for breast cancer detection.

In recent years, the global rise in breast cancer incidence has spurred extensive research into IR imaging for breast cancer diagnosis. Prior research has explored thermal imaging for various medical applications, including diabetic foot disease, ocular surface temperature analysis, and tumor detection<sup>1-6</sup> Click or tap here to enter text. Click or tap here to enter text. Click or tap here to enter text. Studies investigating breast cancer detection through thermal imaging have examined bi-spectral invariant features, color segmentation techniques, and deep learning-based segmentation methods<sup>7-14</sup> Click or tap here to enter text. Click or tap here to enter text. Click or tap here to enter text. Click or tap here to enter text. A novel method combining rotational thermography and dynamic temperature analysis has been developed to address challenges in breast cancer screening<sup>15-17</sup> Click or tap here to enter text. Click or tap here to enter text. This non-contact, non-invasive approach enhances the visibility of abnormalities in breast tissue, improving detection accuracy. Machine learning algorithms trained on extracted features aid in distinguishing normal from abnormal patterns. Earlier, EtehadTavakol *et al.*<sup>7,10</sup> achieved high detection rates using bi-spectral invariant features and K-means clustering for segmentation.<sup>7,10</sup> Garduño-Ramón *et al.*<sup>11</sup> introduced a non-invasive tool utilizing temperature and texture features, yielding promising results<sup>11</sup> Various segmentation techniques, including K-means, fuzzy c-means (FCM), and expectation-maximization (EM) algorithms, have been explored, with the EM algorithm demonstrating superior accuracy<sup>11,12</sup> Click or tap here to enter text. Venkataramani *et al.*<sup>10,13,18-22</sup> proposed a semi-automated method using morphological filtering and thresholding, achieving high sensitivity and specificity.<sup>10,13,18-22</sup> Deep learning-based approaches, such as the level-set method, have shown high accuracy in segmenting suspicious regions in breast thermograms.<sup>9,23,24</sup> Thermal imaging has also been utilized for brain tumor detection, highlighting its versatility in medical diagnostics.<sup>13,20,25-27</sup>

While IR imaging shows promise for breast cancer screening, challenges remain, including standardization of temperature values and the need for trained personnel. IR Imaging researches also focus on optimizing machine learning algorithms, integrating advanced imaging techniques, and exploring novel optimization algorithms for enhanced diagnosis and classification.<sup>28-34</sup>

However, one of the primary challenges lies in establishing precise temperature thresholds to differentiate malignant tumors amidst variations in individual heat sources due to diverse medical and physical conditions. Addressing this challenge is crucial in developing effective breast cancer screening systems. This study presents a novel, non-contact, non-invasive breast imaging method capable of capturing comprehensive abnormalities. Several obstacles confront researchers in the development of IR imaging-based breast cancer screening systems, including the surge in breast cancer cases, the cost and invasiveness of current screening modalities, challenges in tracking malignancy progression, poor visibility of affected anatomical areas, patient discomfort during examinations, and shortages of skilled medical professionals. [Table 1](#) summarizes the earlier works and comparison with the approach used in this study. This research endeavors to overcome these challenges through an efficient data collection process and systematic stages of system development for IR image processing techniques. Conducted at a prominent hospital in northeast India, the study comprises four research phases: Three pilot studies (Phase 1 [PS1], Phase 2 [PS2], and Phase 3 [PS3]) and a final study (FS). The study evolves to optimize imaging quality by transitioning from low-resolution forward-looking IR (FLIR) SC-325 cameras in the initial phases to Infratec HD 600 and FLIR T-650 cameras in subsequent phases. The study aimed to develop an efficient and accurate thermal imaging system for breast cancer screening. It progressed through four phases, refining data collection methods and improving imaging results.

In PS1 and PS2, conventional imaging approaches were employed, but challenges such as varied focal lengths and patient movement resulted in unsatisfactory images. PS3 introduced a semi-circular arc for camera movement, allowing for precise focus on one breast at a time, though manual adjustments and open environments presented difficulties. Findings from PS3 and FS underscore the necessity of mounting the IR camera on a motorized mechanical arm capable of rotational thermography, enabling comprehensive imaging coverage. In the final phase (FS), a temperature-controlled chamber and automated hardware and software provided a standardized, touchless, and painless imaging process with an accuracy rate of 93.18% for detecting abnormalities. Data analysis evolved from conventional methods to advanced techniques in PS3 and FS, employing clustering methods and references from ultrasonography (USG) and biopsy reports. Mean temperature and standard deviation analyses further enhance detection precision. The study included diverse breast cancer subtypes and stages, demonstrating the system's applicability across various scenarios. Control groups provided benchmarks for assessing accuracy and

**Table 1. A summary table of earlier works and a comparison with our approach**

Study	Findings	Pros	Cons	Uniqueness of our study
Etehad Tavakol <i>et al.</i> <sup>7,10</sup>	High detection rates using bi-spectral invariant features and K-means clustering for segmentation. <sup>7,10</sup>	High detection rates; effective segmentation technique.	Limited scope; may lack versatility across different conditions.	Our study expands on bi-spectral invariant features with more advanced machine learning algorithms.
Garduño-Ramón <i>et al.</i> <sup>11</sup>	Non-invasive tool utilizing temperature and texture features, yielding promising results. <sup>11</sup>	Non-invasive; promising outcomes.	May require further optimization for diverse cases.	Our study includes more precise temperature controls and advanced segmentation techniques.
Various segmentation techniques	K-means, fuzzy c-means, and EM algorithms were explored, with EM showing superior accuracy. <sup>11,12</sup>	Superior accuracy with EM algorithm.	May face challenges in real-time applications.	Our study integrates advanced techniques, including fuzzy c-means clustering, for better real-time outcomes.
Venkataramani <i>et al.</i> <sup>10,13,18-22</sup>	Semi-automated method using morphological filtering and thresholding, achieving high sensitivity and specificity. <sup>10,13,18-22</sup>	High sensitivity and specificity.	Semi-automated methods may still require human intervention.	Our study uses a fully automated approach with robotic arm movement and data processing.
Deep learning-based approaches	High accuracy in segmenting suspicious regions in breast thermograms. <sup>9,23,24</sup>	High accuracy in segmentation.	Deep learning models may require large datasets for training.	Our study applies machine learning in tandem with a novel data collection protocol for more comprehensive results.
General challenges in IR imaging	Standardization of temperature values; need for trained personnel; variability in individual heat sources. <sup>28-34</sup>	Promising results in detecting abnormalities.	Difficulty in establishing precise temperature thresholds.	Our study introduces a non-contact, non-invasive approach with precise temperature control for improved results.

Abbreviations: EM: Expectation-maximization; IR: Infrared.

specificity. Neural network (NN) parameters and pattern recognition tools assessed the system's performance with high accuracy rates across different phases.

## 2. Data and methods

### 2.1. Data collection

In PS1, data collection was undertaken following the technique previously described in the literature.<sup>14,35</sup> The subject was seated in front of the camera with both hands raised upward, as illustrated in [Figure 1A](#). In PS2, the subject was seated similarly to PS1 with two cameras deployed at two corners for IR image acquisition.<sup>14,30,36</sup> [Figure 1B](#) illustrates the setup for the same.

Several modifications were carried out in the imaging process based on the doctors' guidance. One modification was placing a camera in a fixed position with the patient seated on a rotating chair. In this case, images were acquired from various predetermined angles. The data collection angles are 0°, 30°, 60°, 90°, 120°, 150°, and 180° from the initial position. Since the patient was rotating, focusing on a specific breast was challenging. It also led to a shifting region of interest (ROI) in the images. This variation in focal length led to unsatisfactory imaging results.

The subsequent logical adaptation was repositioning the camera while keeping the patient stationary. However, a significant challenge arose in obtaining a clear IR image

of the breast from a particular angle, as the camera movement and rotation caused the images to overlap. This resulted in the inner quadrant of one breast's IR image being superimposed by the other breast's outer quadrant.

Accordingly, a significant modification was made to address this concern in PS3, as illustrated in [Figure 1C](#). The patient was seated in a fixed position, and the camera moved in a semi-circular arc on an arm-based arrangement. A tabletop mechanical arrangement was developed to ensure that only one breast was focused at the pivot point of the semi-circular arc. The second breast was isolated from the camera view by covering it with an IR-proof barrier. A tabletop setup of PS3 is shown in [Figure 2](#).

Finally, rotational thermography was set up in the FS. A camera rotated in a semi-circular arc and stopped at different angles, with the patient seated in a fixed position. The arrangement is illustrated in [Figure 3](#).

It comprises an enclosed chamber with a breast-shaped grooved hole through the chamber wall. The patients' breasts are positioned one at a time through this hole for IR imaging. The distance from the camera to the subject is 1 m, the minimum focus distance of the IR camera calibrated by the manufacturer at a thermal laboratory. The ground clearance of the system was 0.76 m. A total of 32 thermal IR images were acquired for each subject, with 16 images acquired at a higher ambient temperature, for example,

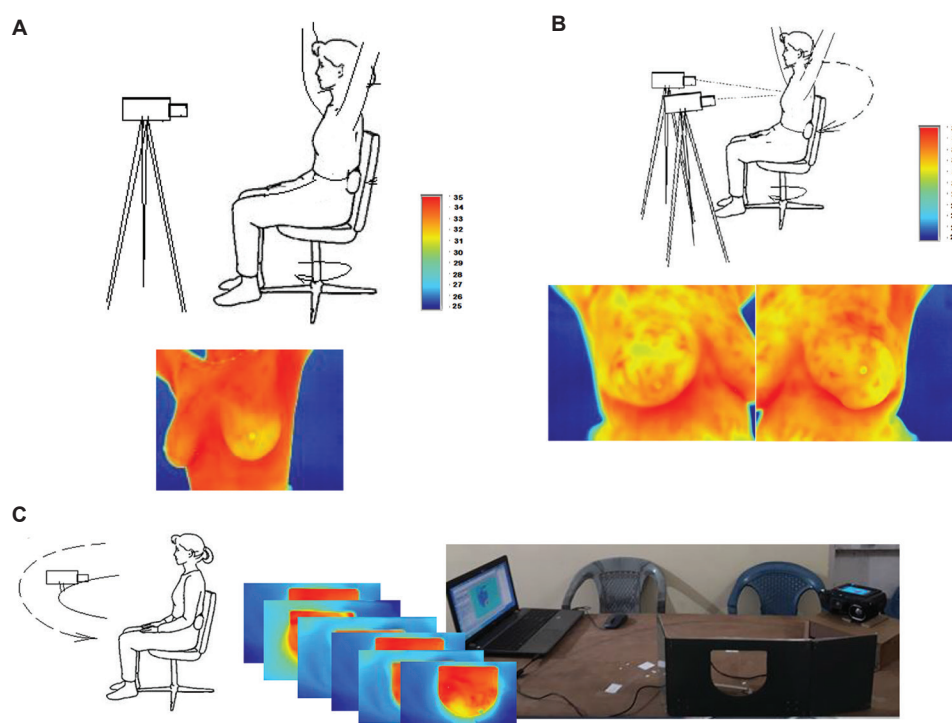


**Figure 1.** Illustration of different patient sitting positions during phases. (A) Data acquisition in Phase 1 with a sample infrared (IR) image. Infrared images were collected using a single IR camera while the patient sat on a rotating chair. (B) Data acquisition in Phase 2 with a sample IR image collected using a dual infrared camera while the patient sat on a rotating chair. (C) Data acquisition setup in Phase 3. Infrared images were collected using a single IR camera while the patient sat on a chair. The camera setup rotated on a tabletop setup. Note: Infrared images shown here were collected during data collection. Illustrations were created using MS Paint.

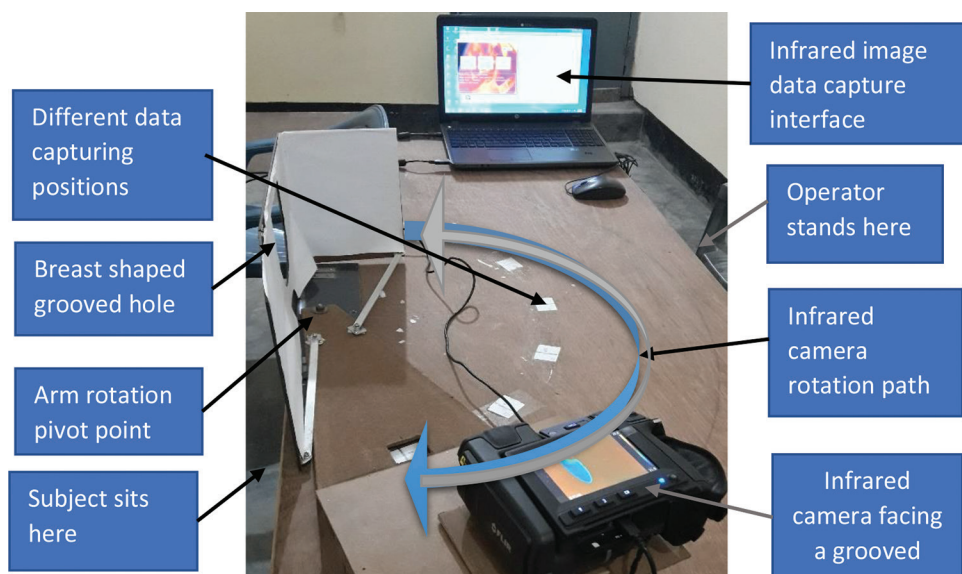


**Figure 2.** Table-top setup for rotational thermography (Phase 3). The setup images shown here were collected during data collection.

25°C, and the other 16 at a lower ambient temperature, for example, 23°C. The temperature variation between the two ambient conditions was 2°C. The IR images were acquired every 30° from 0 to 180°.

Initially, 14 IR images (seven for each breast) and two from the axilla (one from each side) were taken from each IR image set at a particular ambient temperature. During data collection, 17 steps were taken to position and focus



the camera at a particular angle to capture the required IR breast images. These steps are detailed in Table 2. After allowing the ambient temperature to reduce by 2°C through the temperature controller of the air conditioner (AC), the second set of data was acquired. Accordingly, 32 IR breast images were collected over both ambient temperatures. This method is termed dynamic temperature-based data collection.

Protocol-wise, the room temperature is adjusted for each subject in the FS. Controlling the room's temperature and maintaining it at a specific value effectively and quickly was difficult for each patient. The tabletop rotating mechanical setup placed the IR image-capturing system in an airtight chamber to overcome this problem. The temperature inside this chamber was externally regulated through a portable AC. The room temperature was maintained at a constant value through the room AC. This setup is shown in Figure 4.

## 2.2. Data analysis

In thermal imaging, the camera is the primary device for acquiring the data to be analyzed for breast cancer screening. While previous studies are based on this methodology, their technique is different and not in consonance with the

imaging system to generate appropriate images considering variations in temperature and other physical conditions that influence imaging. Hence, detailed knowledge and appropriate system adaptation are essential. Without such intelligent data collection processes, data analysis is crucial for algorithmic perfection and improved machine learning performance.<sup>9,11</sup> Therefore, integrating data collection and analysis while exploring the impact of environmental conditions on IR imaging is essential and required at every step for optimal system performance.

While some researchers have developed data collection protocols, the data analysis algorithms are unsuitable for integration with IR image processing techniques, resulting in poor execution for the breast cancer screening system. This study integrated IR image processing techniques into the system at every stage, leading to efficient system development and gradual software evolution. This results in an effective IR image processing algorithm. Previous studies used online databases like Thermalytix<sup>37</sup> to develop IR imaging algorithms. However, its real-life implementation had a limitation as this database needs more information for such development. Therefore, a novel data collection protocol was developed and implemented in the FS to overcome this limitation.

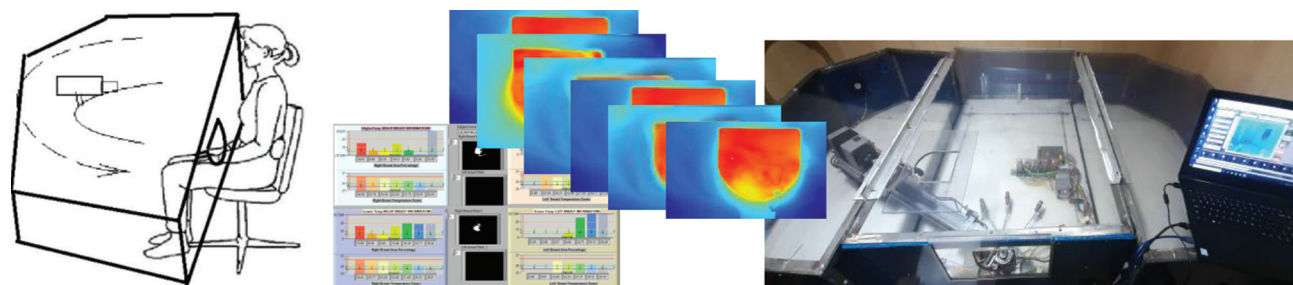


**Figure 3.** Rotational thermography setup in the final study consisting of an infrared camera in a temperature-controlled enclosure. Infrared images were collected using a single infrared camera while the patient sat on a chair. The camera setup rotated on a tabletop setup that was enclosed by a temperature-controlled chamber. The infrared images shown here were collected during data collection. Illustrations were created using MS Paint

**Table 2.** Details of the research phases and evolution to the final stage

Phase	Description	No. of patients	Design setup	Challenges/observations
PS1	Two low-resolution cameras were used for image acquisition from 45° angles.	71	Subject is seated in front of the cameras with raised hands.	Skilled personnel are required for data collection and analysis.
PS2	A single camera was fixed, and images were acquired from various angles while the patient was seated on a rotating chair.	10	Fixed camera setup with a rotating chair.	Challenging to focus on a specific breast due to patient rotation.
PS3	Exploration of different positioning techniques in an open space air-conditioned room.	33	Semi-circular camera movement with one breast focused and the other covered.	Manual hardware movement and difficulty in controlling ambient temperature.
FS	Rotational thermography in a temperature-controlled chamber.	88	Rotating camera in a semi-circular arc.	Automated hardware movement and standardized protocol in an enclosed environment.

Abbreviations: FS: Final study; PS: Phase.

### 2.3. IR-image feature-based analysis technique

In PS1 and PS2, the IR images were analyzed conventionally, following the method adopted in previous studies. The features extracted were the mean, median, mode, standard deviation, histogram, and maximum value. Analysis was conducted in consultation with doctors, but no reference was made to IR images acquired through USG, mammography, or biopsy.

In PS3, the primary reference source was the USG and biopsy reports obtained through other modalities. IR image-based clustering was used for image segmentation and to extract the ROI.

The mean temperature of each ROI, interpreted as different body temperature zones, was used as the discriminating feature. IR image K-means clustering was used for clustering the other image features.<sup>12,25,28</sup> The clustering method was gradually improved, and the number of clusters was optimized from 20 to seven based on experimental validation by consulting doctors based on abnormalities found in the USG and biopsy reports. This study extracted temperature-based clustering features for IR image segmentation for 33 subjects.<sup>8</sup> In the next stage of development (FS), the image background and foreground were separated through FCM clustering.<sup>7</sup> Figure 5 shows the variation in the IR breast images captured from different angles, with the abnormality detected by the software and doctors as irregular and box-shaped ROI, respectively.

Final IR image analysis was accomplished after integrating the temperature-controlled enclosure into the system. The higher ambient temperature state was chosen as the reference temperature. The ROI was divided into seven clusters through K-median clustering and was defined as the features in the machine learning algorithm for processing. Seven clusters were finalized based on experimental validation of the abnormality found in the USG and biopsy reports by the consulting doctors.

Subsequently, another dataset was acquired in the lower ambient temperature state. The differences between the two datasets were the key discriminating features for analysis. This novel analysis technique was tested on 88 subjects from a hospital in northeast India. Figure 6 displays the frontal view of the IR images of a subject's affected and normal breasts, highlighted by the red and blue zones, respectively.

#### 2.3.1. Temperature area clustering method

The number of pixels corresponding to each temperature cluster zone was recorded during IR image analysis. The total number of pixels represented the area of each zone. For example, the camera used in this study captures a  $640 \times 480$ -pixel IR image, which is considered to be 100% area. Accordingly, if a particular zone had 7962 pixels, it spread over 2.59% of the IR image and was known as a percent area cluster. The distributions of these area zones across different temperatures are depicted in Figure 7 using bar plots. Higher temperature regions indicative of abnormalities are conventionally represented in specific colors. The color scale in the figure does not mark the seven cluster zones described in this paper. Instead, it only demonstrates the color temperature relative to the IR image, while the clusters are outlined plots overlaid on the IR image.

Figure 7 illustrates the real-world implications of the temperature zone versus percent area cluster analysis. For the patient in question, imaging at a higher ambient temperature revealed that the right breast had 14.91% of its area at  $34.59^\circ\text{C}$  (zone 0). When the ambient temperature was lowered, the area of the right breast at  $34.43^\circ\text{C}$  increased to 15.89% (zone 0). Since the highest body temperature did not decrease with a change in ambient temperature, we concluded that the right breast had an abnormality. Conversely, for the left breast, the highest temperature at a higher ambient temperature was  $33.50^\circ\text{C}$ , covering 0.59%

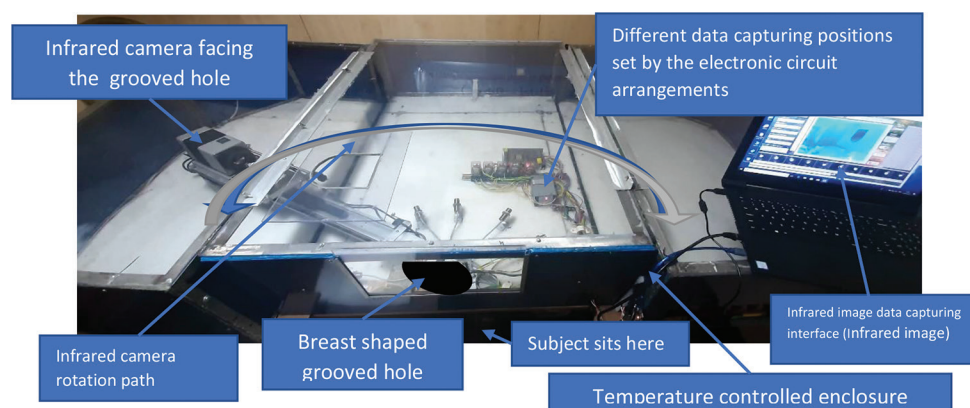
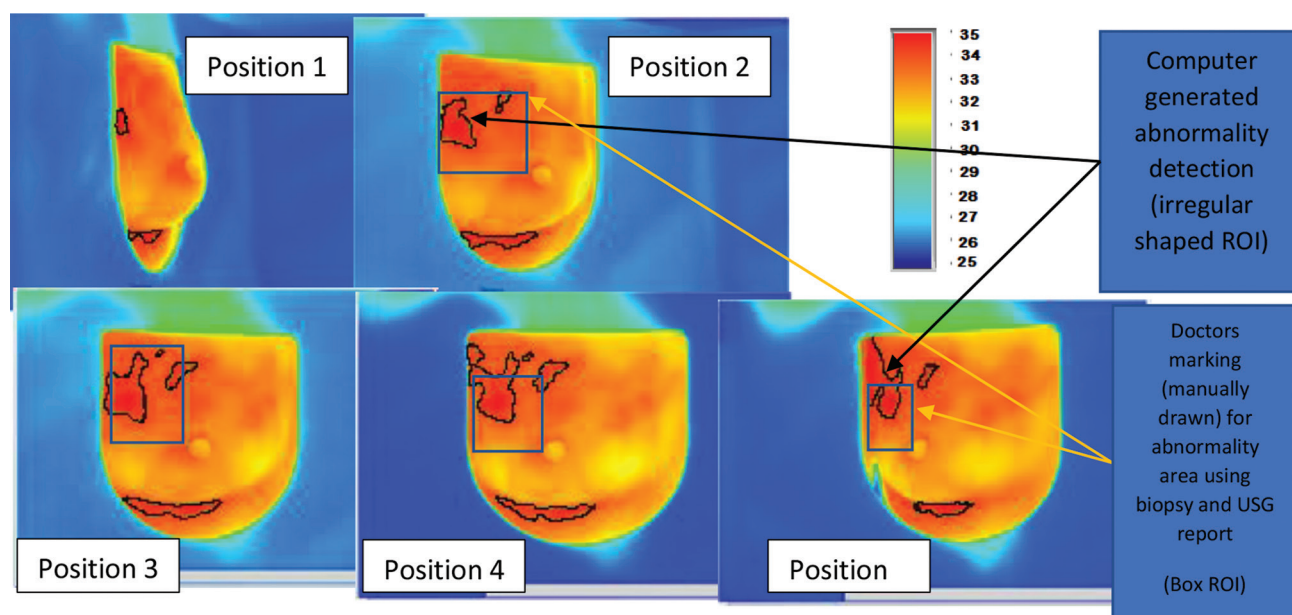
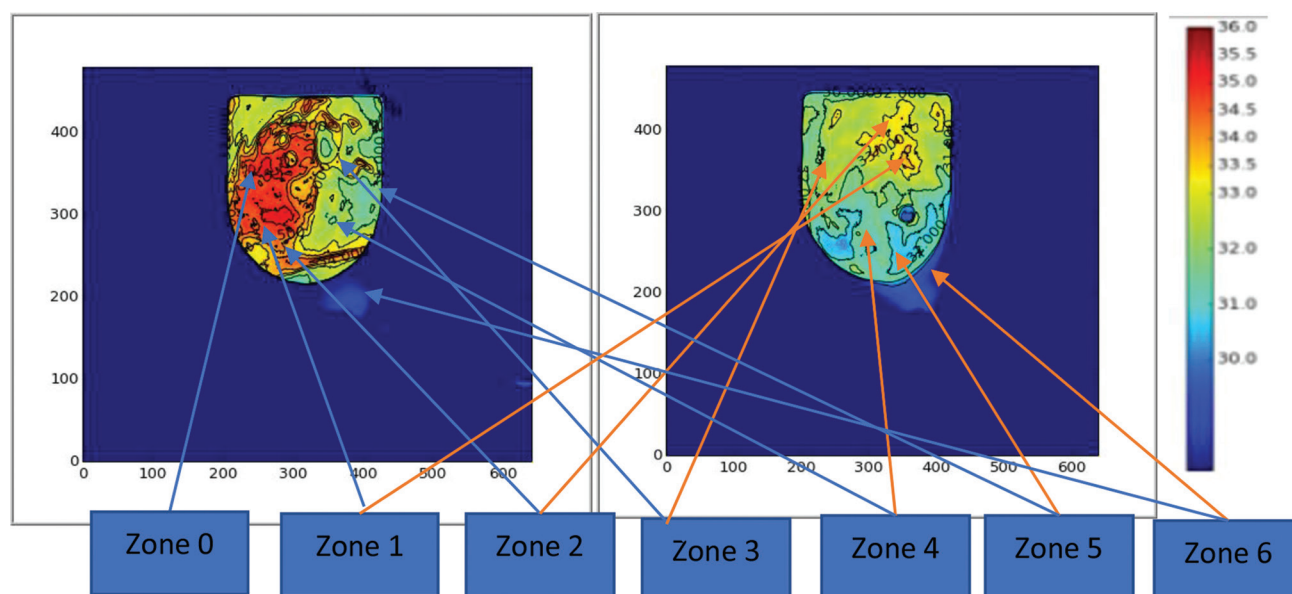


Figure 4. Rotational thermography setup in a temperature-controlled enclosure. Setup images shown here are collected during data collection



**Figure 5.** Region of interest of detected abnormality on infrared breast images captured from different angles. Infrared images shown here were collected during data collection. Illustrations were created using MS Paint. Abbreviation: USG: Ultrasonography.



**Figure 6.** Frontal view of the infrared images of the affected (right) and normal (left) breast. Infrared images shown here were collected during data collection. Illustrations were created using MS Paint.

of the area (zone 1). While the ambient temperature was lowered, 0% of the area was at that temperature (zone 1). Instead, the highest temperature was shifted to zone 2, which dropped to 0.70% of the area. This implies that the body temperature of the left breast significantly decreased with a change in ambient temperature, implying no abnormality.

The temperature area clustering method and its related algorithm were implemented through LabVIEW, which has been copyrighted. Utilizing the LabVIEW environment for image analysis and validation through clinical summary reports, this study introduces an intelligent data collection protocol to enhance system performance, building upon previous research. Ethical approval from the Cachar Cancer



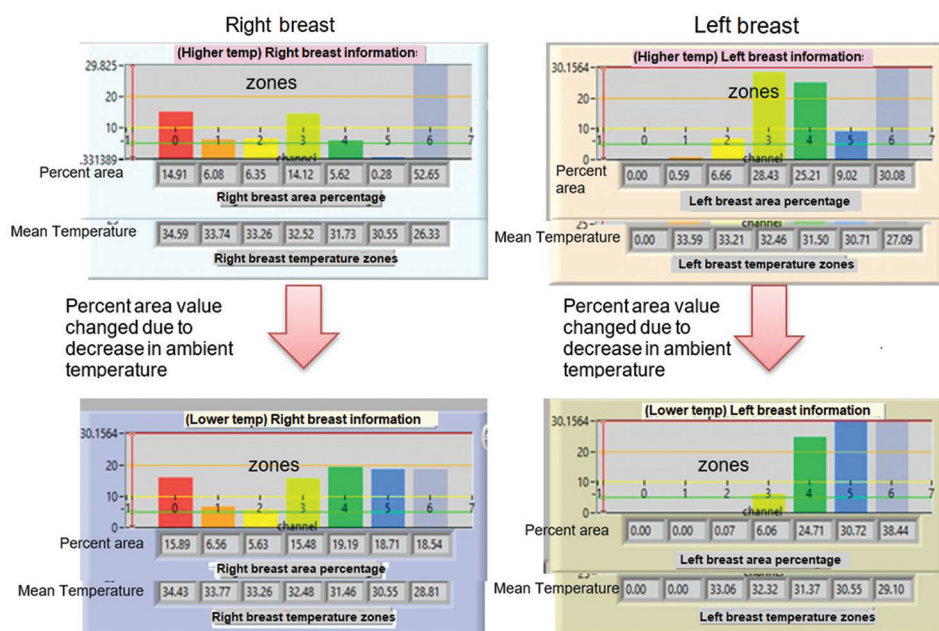


Figure 7. Percent area and temperature zone for two ambient temperatures. Illustrations were created using MS Paint. Abbreviation: Temp: Temperature.

Hospital and Research Centre IRB/Ethics Committee ensures adherence to rigorous ethical standards in research conduct.

### 3. Results and discussion

#### 3.1. Result A

The study aimed to develop an efficient and accurate imaging system for breast cancer screening using thermal imaging techniques. Four phases were conducted to refine the data collection process and improve imaging results. The challenges and observations encountered in each phase led to the development of a more advanced and reliable system in the FS.

In PS1, data acquisition utilized two low-resolution FLIR cameras. The patients were seated in front of the cameras with both hands raised upward. Fixed angulated images were taken from a 45° angle. Skilled personnel were required for data collection and analysis, making it a human-dependent process. This approach provided initial insights into the use of thermal imaging for breast cancer screening.

In PS2, a similar setup to PS1 was used, but with one FL SC325 camera, and angular views were captured. The camera was fixed while the patient sat on a rotating chair, and images were acquired from various predetermined angles. However, the patient's rotational movement made it challenging to focus on a specific breast, leading to

variations in focal length and unsatisfactory imaging results.

To address these challenges, PS3 introduced rotational thermography. The patient was seated in a fixed position, and the camera moved in a semi-circular arc on an arm-based arrangement. A tabletop mechanical setup ensured that only one breast was focused at the arc's pivot point while the other breast was covered with an IR-proof barrier. This modification improved control and focus on a single breast, improving imaging results. However, manual hardware movement and data collection in an open-space environment pose difficulties in maintaining reliable and standardized data.

Finally, in the FS phase, a temperature-controlled chamber was introduced to overcome the challenges faced in previous phases. The camera was set to rotate in a semi-circular arc and stop at various angles while the patient remained fixed. The enclosed chamber provided a controlled environment for data collection, eliminating the need for manual temperature control. Thirty-two thermal IR images were captured for each subject at higher and lower ambient temperatures. This phase employed robotic arm-based automated hardware movement and an automated software analysis tool, resulting in a standardized protocol and improved data collection system.

The proposed imaging system showcased several salient features, including a touchless and painless process for maximum patient comfort, a rotating gantry for acquiring



different angles of the breast, dynamic IR image collection in a temperature-controlled enclosed chamber, and a simplified user interface for data collection, analysis, and interpretation.

Regarding data analysis techniques, PS1 and PS2 followed conventional methods used in previous studies. Features such as mean, median, mode, standard deviation, histogram, and maximum value were extracted from the IR images. However, no reference was made to images acquired through other modalities, such as USG, mammography, or biopsy. The PS3 and FS are complete with the information about PS1 and PS2, assessed for their value in the research article.

In PS3, a shift toward a more comprehensive analysis technique was observed. The primary reference source became the USG, and biopsy reports were obtained through other modalities. IR image-based clustering was employed to segment and extract the ROI. The mean temperature of each ROI was used as a discriminating feature, and K-means clustering was applied to cluster other image features. The clustering method was gradually improved, and the number of clusters was optimized based on experimental validation and consultation with doctors.

The FS phase enhanced the data analysis technique by separating the image background and foreground through FCM clustering. This allowed for better detection and delineation of abnormalities in the IR breast images. The collaboration between software analysis tools and medical experts resulted in identifying irregularly shaped and box-shaped ROIs as potential abnormalities, as shown in Figure 5.

The study demonstrated the importance of integrating data collection and analysis techniques to improve the performance of breast cancer screening systems using IR thermography. The iterative improvements in the data acquisition setup and analysis algorithms led to a more standardized and efficient process. With its temperature-controlled chamber, rotating camera setup, and automated analysis tools, the FS phase showed promising results for accurate and reliable breast cancer screening.

The data presents a comprehensive overview of breast cancer subtypes, sizes, and stages within the examined cohort, providing valuable clinical context. The subtype's distribution includes 63% for ductal carcinoma *in situ*, 25% for invasive ductal carcinoma, 8% for invasive lobular carcinoma, and 4% for other subtypes. Cancer sizes ranged from 0.8 cm to 5.6 cm, with an average size of 2.3 cm. Regarding cancer stages, 42% were Stage I, 33% were Stage II, 15% were Stage III, and 10% were Stage IV. These insights into the cohort's diversity enhance the system's applicability

across various breast cancer scenarios. Table 3 displays the patient data table with all the patients' demographics and the disease stage.

In terms of control, the study employed a comprehensive diagnostic approach, including comparisons between symptomatic and asymptomatic patients, various imaging techniques, and cross-referencing with other diagnostic methods. This control approach thoroughly assessed the system's performance and reliability in different clinical contexts.

Healthy patients were recruited as controls, providing a benchmark for assessing the system's accuracy and specificity. Their demographics included a diverse range of ages and breast health statuses, reflecting the general population and allowing for a comprehensive evaluation of the system's performance across different patient profiles.

The correlation between temperature and readouts is critical for evaluating the breast cancer screening system using IR thermography. Analyses of mean temperature and standard deviation showed the system's ability to identify potential abnormalities based on temperature variations in breast tissue. Improved clustering techniques in later phases enhanced the precision of detecting abnormalities. Overall, the positive correlation between temperature and readouts highlights the system's potential as an effective diagnostic tool for breast cancer screening.

### 3.2. Result B

A meticulous qualitative statistical analysis evaluated abnormality detection accuracy in the captured IR images. Table 4 comprehensively summarizes the detected abnormalities and their corresponding accuracy percentages for each study phase. Notably, a progressive enhancement in accuracy was observed throughout the study duration, with PS3 and the final stage (FS) achieving

**Table 3. Patient data table with all the demographics of the patients and the stage of disease**

Category	Percentage	Details
Subtypes	63	Ductal carcinoma <i>in situ</i>
	25	Invasive ductal carcinoma
	8	Invasive lobular carcinoma
	4	Other subtypes
Tumor sizes	Range	0.8 – 5.6 cm
	Average	2.3 cm
Stages	42	Stage I
	33	Stage II
	15	Stage III
	10	Stage IV

**Table 4. Comparison of studies in the population-based case-control study**

Phase	Data collection	Number of subjects	Mode	TP	TN	FP	FN	Sensitivity (%)	Specificity (%)	Accuracy (%)
PS1	During June 2015 – June 2016	71	Manual	This study was not done on preliminary collected dataset						
PS2	During June 2016 – Aug 2016	10	Manual	1	6	2	1	50%	75%	70%
PS3	October 2017	33	Semi-automated	9	19	4	1	90.00%	82.61%	84.84%
FS	November 2017 – September 2019	88	Automated	23	59	1	5	82.14%	98.33%	93.18%

Abbreviations: EM: Expectation-maximization; FN: False negative; FP: False positive; FS: Final study; IR: Infrared; PS: Phase; TN: True negative.

notably higher detection rates compared to the initial phases (PS1 and PS2). These findings underscore the efficacy of the developed system in identifying potential abnormalities indicative of breast cancer.

In PS1, involving a cohort of 71 patients, the system detected 23 abnormalities. This phase used a manual evaluation process, and a case-control-based study was not conducted. In PS2, with a smaller sample size of 10 patients, the system detected five abnormalities, resulting in an accuracy rate of 70%. The sensitivity in this phase was 50%, meaning half of the actual positives were correctly identified, and the specificity was 75%, indicating a better performance in correctly identifying true negatives. The calculated area under the receiver operating characteristic curve (AUC) for this phase is 0.625. Despite the reduced sample size, the system demonstrated promise in identifying abnormalities.

PS3 marked a significant advancement, encompassing 33 patients. The system detected 30 abnormalities, yielding an impressive accuracy rate of 84.84%. The sensitivity was 90%, highlighting the system's enhanced ability to identify actual positives correctly. The specificity improved to 82.61%, indicating fewer false positives. These metrics underscore the advancements in positioning techniques and enhanced image quality. The calculated AUC for this phase is 0.863, showcasing significant overall discriminative power in distinguishing between positive and negative cases. Phase 4 (FS), involving 88 patients, exhibited the highest performance with an accuracy rate of 93.1%. The sensitivity was 82.14%, showing a high true positive rate, and the specificity reached 98.33%, indicating an excellent true negative rate. These results underscore the system's capability to identify potential abnormalities indicative of breast cancer. This phase illustrates the system's reliability and effectiveness, providing a promising tool for early detection and enhancing patient outcomes. The calculated AUC for this phase is 0.902, further highlighting the system's discriminative power in distinguishing between positive and negative cases.

The study ensured robust model evaluation by dividing the data into distinct phases (PS3 and FS) for training,

validation, and testing. In PS3, the training set consisted of 23 subjects (368 images), with five subjects (80 images) each for validation and testing. For FS, 62 subjects (992 images) were used for training, while 13 subjects (208 images) each were allocated to validation and testing. This approach allowed for efficient model tuning and performance evaluation on unseen data, improving the model's reliability. The results of the NN tools generated are shown in [Figures 8 and 9](#).

The NN parameters included the distribution of different area zones corresponding to different temperatures. Specifically, the study recorded the number of pixels corresponding to each temperature cluster zone, using this as the area of that zone. The IR images ( $640 \times 480$  pixels) were considered 100% area, and the NN analyzed how different area zones were distributed across the images. The network's parameters included seven zones in two ambient temperatures across 16 images per subject. The NN parameters typically included the number of Layers: Three hidden layers; learning rate: 0.001; optimization function: Adam optimizer. Pattern recognition tools were used for image classification and assessed through confusion matrices for accuracy and performance validation. The study employed 5-fold cross-validation as the validation technique for machine learning algorithms, ensuring a thorough and reliable evaluation of the model's performance. This method involves dividing the data into five subsets and training the model 5 times, each using a different subset as the validation set and the remaining subsets as the training set. This approach allowed for a comprehensive evaluation of the NN's ability to identify abnormalities.

Furthermore, mean temperature and standard deviation analysis were conducted to assess the stability and variation of temperature measurements across different phases. Mean temperature was calculated as the sum of individual temperatures divided by the total number of subjects, providing insights into temperature stability. On the other hand, standard deviation offered valuable information regarding temperature variation within the dataset.

The confusion matrices in [Figures 8 and 9](#) show the classification outcomes of the NN pattern recognition tool



**Figure 8.** Neural network classification results of the training and testing datasets for breast abnormality detection for PS3 (33 subjects). The results illustrate model tuning and performance evaluation. The image was created using Matlab software. Abbreviations: CE: Cross-entropy; %E: Percentage of correctly classified elements.

for population-based case-control studies in PS3 and FS, respectively. These matrices offer a visual representation of the classification performance, aiding in assessing the system's accuracy and reliability.

The developed system's exceptional accuracy for screening breast abnormalities and detecting malignant tumors was validated at 93.18%, underscoring its reliability and effectiveness.

Finally, Table 4 provides a comparative analysis of studies conducted in population-based case-control settings, elucidating the progression and refinement of the system across different phases. This comprehensive comparison offers insights into the system's evolution and performance enhancements.

## 4. Discussion

This system has been installed at a renowned hospital in North-east India, known for its mass screening capabilities. The subsequent product deployment will include installations at various hospitals across India, leveraging the system's superior performance and excellent output based on the second dataset acquired through our proposed IR image acquisition and analysis technique.

The study utilized a double-blind validation method where expert doctors and reviewers provided both quantitative and qualitative feedback. This approach ensured an impartial evaluation of the model's performance, as the experts and reviewers were unaware of the algorithm's predictions during the assessment. The





**Figure 9.** Neural network classification results of the training and testing datasets for breast abnormality detection for the final study (88 subjects). The results display model tuning and performance evaluation. The image was created using Matlab software. Abbreviations: CE: Cross-entropy; %E: Percentage of correctly classified elements.

method was rigorously applied across all 88 subjects in the FS phase.

Focused on IR imaging, the study recorded the number of pixels corresponding to each temperature cluster zone and used this information to quantify areas of interest. Given the  $640 \times 480$ -pixel IR images, each subject's dataset included seven zones across two ambient temperatures for 16 images (total number of image data =  $[71 \times 2] + [10 \times 4] + [33 \times 32] + [88 \times 32] = 4054$ ).

The study's primary focus was to explore innovative IR imaging techniques and related features for breast cancer screening. We aimed to investigate temperature-based imaging and machine-learning algorithms as alternative diagnostic methods. This approach allowed us to detect thermal patterns and variations that could indicate potential

abnormalities, providing a different perspective on breast cancer screening. Although integrating these traditional measures could enhance the study, our concentration was on advancing the field of IR imaging to contribute valuable knowledge to breast cancer screening.

The system's repeatability was confirmed by imaging the same breast 5 times, demonstrating high consistency with minimal variability. Results across trials were consistent, as evidenced by acceptable statistical measures, including standard deviation and coefficient of variation, affirming the system's accuracy and clinical viability for breast cancer screening.

Clinical implications and utility: the findings regarding their clinical implications and the system's utility in breast cancer diagnosis and population screening have been

explored. Results indicate the system's promise as an effective diagnostic tool for early detection of high-risk individuals. The system's non-invasive and non-contact nature makes it well-suited for population screening, despite challenges with ambient temperature adjustments.

After considering the experts' concerns, we conducted a thorough comparative analysis, including using the system with biopsy and USG. This analysis was carried out with great attention to detail. This analysis addresses the expert's and concerned doctors' request for a comparison with established diagnostic methods. The system exhibited a sensitivity comparable to that of biopsy (90.2% vs. 88.6%) and USG (90.2% vs. 89.7%). Furthermore, the system displayed competitive specificity, with respective values of 82.8%, 84.6%, and 82.4% for biopsy, USG, and the system. This comprehensive analysis not only addresses reviewers' concerns but also underscores the potential utility of the system as a valuable diagnostic tool.

## 5. Conclusion

IR imaging plays a crucial role in various medical applications, emphasizing IR image acquisition techniques. This paper reported different types of IR image acquisition systems based on trials in a hospital setup and conclusively identified the superior one. Key features of the proposed imaging system include a touchless and painless IR camera-based system for maximum patient comfort; gantry rotation for acquiring multiple breast angles; dynamic IR image collection within a temperature-controlled chamber; and a simplified user interface for data collection by technicians, IR image analysis experts, and doctors.

The primary challenge in this study was managing patients with varied health conditions. During the early stages of development, patients had to wait a long time to reach a stable room temperature. However, as the development of the novel data acquisition technique progressed, the evolved system became more user-friendly and efficient regarding imaging quality. The next challenge addressed was maintaining a constant ambient temperature during data collection, which was the most difficult task. It was overcome by implementing a temperature-controllable enclosure. Here, two ambient temperatures have been taken. The higher temperature was 25°C, and the lower temperature was 23°C. The mean temperature adjustment for each subject is 1°C.

Finally, IR image analysis software was developed, incorporating machine learning algorithms that produced excellent results. These findings were cross-validated using USG and biopsy reports. However, several limitations were identified during this study that may have influenced

the results and should be considered when interpreting the findings. One potential source of bias arises from the sample population, which may not fully represent the general population due to demographic variations and differences in breast cancer prevalence, thereby potentially limiting the study's generalizability.

Confounding variables such as variations in breast density, tissue composition, and patient positioning during imaging could have affected the accuracy and consistency of the system. Although the study attempted to control for these factors, they may have introduced some degree of variability in the results. External factors such as equipment quality and maintenance, technician expertise, and interpretation differences among medical professionals may have also impacted the study's outcomes. Moreover, relying on USG and biopsy reports to cross-validate the system's performance introduces potential dependencies on the accuracy and reliability of these other diagnostic modalities.

The study progressed iteratively, with each phase's findings and feedback shaping the design and objectives of the subsequent phase. This approach allowed us to refine methods and address challenges progressively. By enhancing techniques and analyses based on results-driven objectives, each phase naturally evolved, focusing on enhancing the efficiency and accuracy of our breast cancer screening imaging system. In terms of sample size, we acknowledge that the varying sizes across phases may impact the overall consistency of the results. However, the number of subjects available for each phase depended on live patient availability during the study period at the hospital. Practical constraints such as time and resource limitations influenced sample sizes, despite efforts to maintain consistency. While we tried to work with consistent sample sizes, external factors such as patient availability and medical considerations posed challenges. However, our phased approach enabled us to optimize methods and techniques, yielding improved results in each subsequent phase. Our study focused on real-world application and practical implementation, requiring flexibility in our approach.

In addition, the challenges faced during data collection, such as maintaining a constant ambient temperature and managing patients with diverse health conditions, affected the precision and consistency of the imaging process. While we addressed these challenges throughout the study, residual variability may have affected the results. Overall, while the study presents promising findings, we carefully considered its limitations and potential sources of bias when evaluating the system's effectiveness and applicability in broader clinical settings. Future research should address

these limitations to further validate and improve the system.

## Acknowledgments

We sincerely acknowledge Sayantani Banerjee's technical contributions and Dr. R. Ravi Kannan and his team for providing hospital support for data collection and test beds. In addition, Sri Aditya Kumar Sinha, Center Head, C-DAC, Kolkata, has provided constant support and help with the implementation.

## Funding

This project is funded by MeitY (Ministry of Electronics and Information Technology), Government of India, bearing administrative approval No. 1(4)/2015- ME&HI.

## Conflict of interest

The authors declare no conflicts of interest.

## Author contribution

*Conceptualization:* Asok Bandyopadhyay, Himanka S. Mondal

*Investigation:* Himanka S. Mondal, Barnali Pal

*Methodology:* Himanka S. Mondal

*Writing – original draft:* Asok Bandyopadhyay, Himanka S. Mondal

*Writing – review & editing:* Bivas Dam, Dipak C. Patranabis, Asok Bandyopadhyay

## Ethics approval and consent to participate

The study conducted in this paper involved human subjects and was approved by the Cachar Cancer Hospital and Research Centre Institutional Review Board (IRB)/Ethics Committee. The approval number granted by the IRB/Ethics Committee is CCHRC/IRB/01/2019/254. The IRB/Ethics Committee reviewed and approved the study protocol, ensuring compliance with ethical standards and guidelines for research involving human participants. Written informed consent was obtained from each human subject before their participation. The consent form provided detailed information about the study objectives, procedures, potential risks and benefits, confidentiality measures, and the voluntary nature of participation. Subjects were informed of their right to withdraw from the study at any time without consequences. Consent forms were securely stored in compliance with data protection regulations.

## Consent for publication

Participants gave consent to publish their data in the consent paper.

## Availability of data

The data utilized in this study are proprietary to the Ministry of Electronics and Information Technology (MeitY), Government of India. Therefore, it cannot be disclosed due to confidentiality agreements and is not available for external access or disclosure.

## References

1. Sivanandam S, Anburajan M, Venkatraman B, Menaka M, Sharath D. Medical thermography: A diagnostic approach for type 2 diabetes based on non-contact infrared thermal imaging. *Endocrine*. 2012;42(2):343-351.  
doi: 10.1007/s12020-012-9645-8
2. Nishide K, Nagase T, Oba M, *et al.* Ultrasonographic and thermographic screening for latent inflammation in diabetic foot callus. *Diabetes Res Clin Pract*. 2009;85(3):304-309.  
doi: 10.1016/j.diabres.2009.05.018
3. Fujiwara Y, Inukai T, Aso Y, Takemura Y. Thermographic measurement of skin temperature recovery time of extremities in patients with type 2 diabetes mellitus. *Exp Clin Endocrinol Diabetes*. 2000;108(7):463-469.  
doi: 10.1055/s-2000-8142
4. Fushimi H, Inoue T, Yamada Y, Matsuyama Y, Kubo M, Kameyama M. Abnormal vasoreaction of peripheral arteries to cold stimulus of both hands in diabetics. *Diabetes Res Clin Pract*. 1996;32(1-2):55-59.  
doi: 10.1016/0168-8227(96)01222-3
5. Sodi A, Giambene B, Miranda P, Falaschi G, Corvi A, Menchini U. Ocular surface temperature in diabetic retinopathy: A pilot study by infrared thermography. *Eur J Ophthalmol*. 2009;19(6):1004-1008.  
doi: 10.1177/112067210901900617
6. Ring EFJ, Ammer K. Infrared thermal imaging in medicine. *Physiol Meas*. 2012;33(3):R33-R46.  
doi: 10.1088/0967-3334/33/3/R33
7. EtehadTavakol M, Sadri S, Ng EYK. Application of K- and Fuzzy c-means for color segmentation of thermal infrared breast images. *J Med Syst*. 2010;34(1):35-42.  
doi: 10.1007/s10916-008-9213-1
8. Etehadtavakol M, Ng EYK. *Color Segmentation of Breast Thermograms: A Comparative Study*. Singapore: Springer; 2017:69-77.  
doi: 10.1007/978-981-10-3147-2\_6
9. Pramanik S, Banik D, Bhattacharjee D, Nasipuri M, Bhowmik MK, Majumdar G. Suspicious-region segmentation from breast thermogram using DLPE-based level set method. *IEEE Trans Med Imaging*. 2019;38(2):572-584.  
doi: 10.1109/TMI.2018.2867620



10. EtehadTavakol M, Chandran V, Ng EYK, Kafieh R. Breast cancer detection from thermal images using bispectral invariant features. *Int J Therm Sci.* 2013;69:21-36.  
doi: 10.1016/j.ijthermalsci.2013.03.001
11. Garduño-Ramón MA, Vega-Mancilla SG, Morales-Henández LA, Osornio-Rios RA. Supportive noninvasive tool for the diagnosis of breast cancer using a thermographic camera as sensor. *Sensors (Basel).* 2017;17(3):497.  
doi: 10.3390/s17030497
12. Prakash RM, Bhuvaneshwari K, Divya M, Sri KJ, Begum AS. Segmentation of Thermal Infrared Breast Images Using K-means, FCM and EM Algorithms for Breast Cancer Detection. In: *2017 International Conference on Innovations in Information, Embedded and Communication Systems (ICIIECS)*, IEEE; 2017:1-4.  
doi: 10.1109/ICIIECS.2017.8276142
13. Venkataramani K, Mestha LK, Ramachandra L, Prasad SS, Kumar V, Raja PJ. Semi-automated breast cancer tumor detection with thermographic video imaging. *Annu Int Conf IEEE Eng Med Biol Soc.* 2015;2015:2022-2025.  
doi: 10.1109/EMBC.2015.7318783
14. Kandlikar SG, Perez-Raya I, Raghupathi PA, et al. Infrared imaging technology for breast cancer detection - Current status, protocols and new directions. *Int J Heat Mass Transf.* 2017;108:2303-2320.  
doi: 10.1016/j.ijheatmasstransfer.2017.01.086
15. Bandyopadhyay A, Chaudhuri A, Mondal HS. IR based Intelligent Image Processing Techniques for Medical Applications. In: *2016 SAI Computing Conference (SAI)*, IEEE; 2016:113-117.  
doi: 10.1109/SAI.2016.7555970
16. Bandyopadhyay A, Mondal HS, Dam B, Patranabis DC. Efficient infrared image processing and machine learning algorithm for breast cancer screening. *Comput Methods Biomech Biomed Eng Imaging Vis.* 2023;11:2226-2238.  
doi: 10.1080/21681163.2023.2225639
17. Bandyopadhyay A, Mondal HS, Pal B, Dam B, Patranabis DC. Exploring the Potential Use of Infrared Imaging in Medical Diagnosis: Comprehensive Framework for Diabetes and Breast Cancer Screening. In: *Fourth International Conference on Image Processing and Capsule Networks (Lecture Notes in Networks and Systems)*. Springer Nature Singapore; 2023:411-424.  
doi: 10.1007/978-981-99-7093-3\_27
18. Kapoor P, Prasad SVA. Image Processing for Early Diagnosis of Breast Cancer Using Infrared Images. In: *2010 the 2<sup>nd</sup> International Conference on Computer and Automation Engineering (ICCAE)*, IEEE; 2010:564-566.  
doi: 10.1109/ICCAE.2010.5451827
19. Gonzalez RC, Woods RE. *Digital Image Processing*. 4<sup>th</sup> ed. London: Pearson Education, Inc.; 2007.
20. Chen GL, Lee CY. Iterative Morphology-based Segmentation of Breast Tumors in Ultrasound Images. In: *2014 International Symposium on Computer, Consumer and Control*, IEEE; 2014:1107-1110.  
doi: 10.1109/IS3C.2014.288
21. Li C, Xu C, Gui C, Fox MD. Distance regularized level set evolution and its application to image segmentation. *IEEE Trans Image Process.* 2010;19(12):3243-3254.  
doi: 10.1109/TIP.2010.2069690
22. Caselles V, Catté F, Coll T, Dibos F. A geometric model for active contours in image processing. *Numer Math.* 1993;66:1-3.  
doi: 10.1007/BF01385685
23. Mambou SJ, Maresova P, Krejcar O, Selamat A, Kuca K. Breast cancer detection using infrared thermal imaging and a deep learning model. *Sensors (Basel).* 2018;18(9):2799.  
doi: 10.3390/s18092799
24. Tsietso D, Yahya A, Samikannu R. A review on thermal imaging-based breast cancer detection using deep learning. *Mob Inf Syst.* 2022;2022:1-19.  
doi: 10.1155/2022/8952849
25. Wu MN, Lin CC, Chang CC. Brain Tumor Detection Using Color-Based K-Means Clustering Segmentation. In: *Third International Conference on Intelligent Information Hiding and Multimedia Signal Processing (IIH-MSP)*, IEEE; 2007:245-250.  
doi: 10.1109/IIHMSP.2007.4457697
26. Zhang Y, Wu X, He L, et al. Applications of hyperspectral imaging in the detection and diagnosis of solid tumours. *Transl Cancer Res.* 2020;9(2):1265-1277.  
doi: 10.21037/tcr.2019.12.53
27. Lugano R, Ramachandran M, Dimberg A. Tumor angiogenesis: Causes, consequences, challenges and opportunities. *Cell Mol Life Sci.* 2020;77(9):1745-1770.  
doi: 10.1007/s00018-019-03351-7
28. Houssein EH, Emam MM, Ali AA. An efficient multilevel thresholding segmentation method for thermography breast cancer imaging based on improved chimp optimization algorithm. *Expert Syst Appl.* 2021;185:115651.  
doi: 10.1016/j.eswa.2021.115651
29. Houssein EH, Abdelkareem DA, Emam MM, Hameed MA, Younan M. An efficient image segmentation method for skin cancer imaging using improved golden jackal optimization algorithm. *Comput Biol Med.* 2022;149:106075.  
doi: 10.1016/j.combiomed.2022.106075
30. De Santana MA, Pereira JMS, da Silva FL, et al. Breast cancer diagnosis based on mammary thermography and extreme

- learning machines. *Res Biomed Eng.* 2018;34(1):45-53.  
doi: 10.1590/2446-4740.05217
31. Gonçalves C, Leles A, Oliveira L, Guimaraes G, Cunha J, Fernandes H. Machine Learning and Infrared Thermography for Breast Cancer Detection. In: *The 15<sup>th</sup> International Workshop on Advanced Infrared Technology and Applications*. MDPI; 2019:45.  
doi: 10.3390/proceedings2019027045
32. Dixit S, Kumar A, Srinivasan K. A current review of machine learning and deep learning models in oral cancer diagnosis: Recent technologies, open challenges, and future research directions. *Diagnostics (Basel)*. 2023;13(7):1353.  
doi: 10.3390/diagnostics13071353
33. Cohen EE, Ahmed O, Kocherginsky M, *et al.* Study of functional infrared imaging for early detection of mucositis in locally advanced head and neck cancer treated with chemoradiotherapy. *Oral Oncol.* 2013;49(10):1025-1031.  
doi: 10.1016/j.oraloncology.2013.07.009
34. *Advanced Thermography and Preventive Education*. Available from: <https://thermogramcenter.com> [Last accessed on 2023 Dec].
35. Ng EYK. A review of thermography as promising non-invasive detection modality for breast tumor. *Int J Therm Sci.* 2009;48(5):849-859.  
doi: 10.1016/j.ijthermalsci.2008.06.015
36. Wishart GC, Campisi M, Boswell M, *et al.* The accuracy of digital infrared imaging for breast cancer detection in women undergoing breast biopsy. *Eur J Surg Oncol.* 2010;36(6):535-540.  
doi: 10.1016/j.ejso.2010.04.003
37. Kakileti ST, Madhu H, Subramoni T, Manjunath G. Thermalytix: Using AI to save lives. *XRDS Crossroads ACM Mag Stud.* 2020;26(3):38-41.  
doi: 10.1145/3383384